P. V. Nagy*
S. Desa*
Department of Mechanical Engineering

W. L. Whittaker
Field Robotics Center
Carnegie Mellon University
Pittsburgh, Pennsylvania 15213

Energy-Based Stability Measures for Reliable Locomotion of Statically Stable Walkers: Theory and Application

Abstract

To plan safe, reliable walker motions, it is important to assess the stability of a walker. In this article, two basic modes of walker stability are defined and developed: stance stability and walker stability. For slowly moving, statically stable walkers, it is convenient to use the magnitude of the amount of the work required to destabilize a walker as a measure of the stability of that walker. Furthermore, as shown in this article, the compliance of the walker and/or terrain can significantly affect the work necessary to destabilize the walker. Consideration of compliance and the two modes of walker stability leads to the definition and development of four energy-based stability measures: the rigid stance stability measure, the compliant stance stability measure, the rigid walker stability measure, and the compliant walker stability measure. (The rigid stance stability measure is identical to the energy stability margin reported in Messuri and Klein [1985].) Several examples are used to demonstrate the application and use of these stability measures in type selection, gait planning, and control of the walker. The outcome of the present work is a more complete approach to using stability measures to ensure reliable walker gait planning and control.

1. Introduction

There is a growing need for walking robots to traverse natural terrain in applications such as agriculture (Hoffman 1991) and planetary exploration (Bares et al. 1989). These demanding applications require an adequate characterization and quantification of the walker–terrain interaction in order to achieve reliable planning and control of walking (Nagy 1991; Nagy, Desa, and Whittaker 1992; Nagy, Whittaker, and Desa 1992). The "stability" of a walker is one of the important attributes that characterize walker–terrain interaction and must be estimated for the purposes of evaluating the reliability of planned walker motions. Because reliable evaluation of planned motions depends on the accuracy of the stability estimates, meaningful stability measures and methods to compute these measures are needed.

Early stability measures did not consider the complete configuration of the walker and the nature of the terrain. While later work did consider the configuration more completely, the nature of the terrain and certain aspects of the configuration of the walker were still not taken into account. Therefore, the estimates resulting from the use of these measures could easily "over-predict" the stability for the case of the walker traversing compliant terrain, or be too conservative in the case of certain walker configurations (as shown in Section 4 for the case of a frame walker).

This article develops stability measures that are more precise than those that previously existed for statically stable walking machines, thereby providing a tool for improving the reliability of locomotion when properly used in walker design, gait planning, and walker control. The significant new feature of these measures is that they take into account the effect of walker/terrain compliances and walker configuration on the stability of the walker.

1.1. Review of Related Research

A large class of walking machines (or walkers) are designed to have at least four legs. If at least three feet are in ground contact at any time, then these multilegged walkers are called *statically stable walkers* since the ground-contacting feet provide a stable base of support for slow motions of the walker. The stability of such

*Nagy is currently at the Mechanical Engineering Department, Northern Illinois University, DeKalb, Illinois 60115. Desa is currently at the Sibley School of Mechanical and Aerospace Engineering, Cornell University, Ithaca, New York 14850. E-mail: sd@lobe.edrc.cmu.edu
The International Journal of Robotics Research,
Vol. 13, No. 3, June 1994, pp. 272–287.

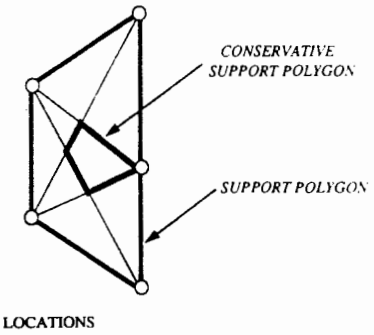

Fig. 1. Plan view of the support polygons for five ground-contacting feet.

slowly moving, multilegged, statically stable walkers is adequately quantified by using static analysis.

Consider a multilegged, statically stable walker with at least three feet in contact with terrain that is not necessarily level. Most stability measures for this class of walker make use of the concept of a "support polygon," which is determined as follows. The locations of all ground-contacting feet are first projected onto a horizontal plane. The *support polygon* (SP) is the convex hull of these projections (McGhee and Frank 1968). An example of a support polygon for five ground-contacting feet is depicted in Figure 1. A walker is stable if and only if the projection of the center of gravity (c.g.) of the walker onto the same horizontal plane lies inside the support polygon. In such cases, the support polygon is referred to as a *stable support polygon*. One of the first attempts to quantify stability defined the "stability margin" as the shortest (horizontal) distance between the projected c.g. location and the edges of the support polygon (Zhang and Song 1989).

To take into account the possibility of support failure of a single leg, Mahalingham and Whittaker (1989) defined the *conservative support polygon* (CSP), which is determined as follows. If there are n ground-contacting feet whose projections form the support polygon, then n subsets of the support polygon can be formed as follows. Each subset is the convex hull of the projections onto a horizontal plane of one of the n possible combinations of $(n - 1)$ of the feet that form the support polygon. The intersection of these n subsets forms the conservative support polygon. The CSP for a typical set of five ground-contacting feet is shown in Figure 1 along with the corresponding support polygon. To quantify stability with respect to the CSP, the conservative stability margin is defined as the shortest (horizontal) distance between the projected c.g. location and the edges of the conservative support polygon.

The stability margin and the conservative stability margin only consider the projection of the ground-contacting feet and c.g. location of the walker onto a horizontal plane. However, the height of the c.g. and the differences in the terrain elevations of ground-contacting feet have a significant impact on the stability of a walker. For example, a walker tends to be more stable as its c.g. is lowered, and less stable as the grade of the terrain being traversed increases (i.e., becomes steeper). To take walker configuration more fully into account, Messuri and Klein (1985) proposed the *energy stability margin* (ESM). The ESM, also discussed in Song and Waldron (1989), is simply the minimum work that must be done on a walker to tip it over an edge of the support boundary.[1] The ESM, therefore, is a better measure of the stability of the walker configuration than the stability margin.

1.2. Outline of the Contents

The ESM, derived in Section 3 in a new form necessary for our development, provides a good estimate of the stability of a walker for the case of a rigid walker on rigid terrain. Since, in the present context, we distinguish between several energy-based stability measures, the ESM is more appropriately referred to as the *rigid stance stability measure* (RSSM), as it is used to evaluate the stability of a given stance of a rigid walker on rigid terrain (Section 3). To consider the effects of compliant terrain on the stability of a walker, the RSSM is extended to develop the *compliant stance stability measure* (CSSM) in Section 4. The RSSM is then further extended to include the possible stabilizing effects of feet that are not in ground contact, giving rise to the *rigid walker stability measure* (RWSM) and *compliant walker stability measure* (CWSM) for rigid and compliant terrains, respectively (Section 5).

Having developed a set of useful stability measures, the proper use of these measures is discussed in Section 6. The choice of the appropriate stability measure is clarified using two actual types of walkers and two types of terrain. A systematic procedure for choosing the proper stability measure is then presented. The use of stability measures in walker design, gait planning, and control is also discussed. Section 7 summarizes our work and draws appropriate conclusions.

2. Terminology

The *stance* of a walker is the configuration of the walker, including the location of its center of gravity and the location of each foot with respect to the terrain. Associated

1. The support boundary is the boundary formed by line segments between adjacent feet whose vertical projections comprise the support polygon. The projection of the support boundary onto a horizontal plane is the support polygon.

with a given stance of the walker, there exists a unique support polygon. If the support polygon is stable, then the given stance is said to be stable. In the sequel, the given or specified stance is assumed to be stable. From the viewpoint of planning reliable motions, it is necessary to be able to assess how stable the stance is. For this purpose, it is useful to visualize the walker as being acted upon by a "disturbance" that tries to destabilize it. An unexpected collision of a leg against the terrain or failure of the support below a foot are examples of typical disturbances in the actual operation of a walker.

A stance "fails" when there is a change in the support polygon that is unplanned (i.e., caused by a disturbance). An unexpected change in the support polygon can have one of two consequences: either a new stable support polygon is established, or the walker falls over (and has no stable support polygon). One can therefore distinguish between two types of stability for walkers: stance stability and walker stability. Stance stability corresponds to the ability of the walker to maintain its given stable support polygon. Walker stability corresponds to the ability of the walker to remain in the given (initial) stable stance, or, failing that, to end up in a new stable stance. The unexpected loss of a given stable support polygon will be referred to as *stance instability*. The complete loss of stability when the walker falls over will be referred to as *walker instability*. It is clear that stance instability does not necessarily result in walker instability. However, stance instability is a necessary prerequisite for walker instability to occur.

A measure of the stance stability of a walker is the minimum amount of work that must be "done" by a disturbance in order to destabilize the given stance. A measure of the walker stability is the minimum amount of work that must be "done" by a disturbance in order to topple the walker. Stance stability measures are developed in Sections 3 and 4, while the walker stability measures are developed in Section 5.

3. The Rigid Stance Stability Measure

Because the context of this work is the evaluation of slow, statically stable walking, tipover is modeled as a quasistatic process. The other basic assumptions in this section are that the walker and terrain are rigid and that only legs with feet in ground contact contribute to the stability of the walker. These are the same assumptions that were used in the derivation of the energy stability margin (Messuri and Klein 1985). It is worth noting that while the vertical contact forces exerted by the ground on the feet do depend on the location of the center of the gravity of the walker, these forces do not explicitly affect the stability of the rigid walker on rigid terrain as determined by the stance stability measure.

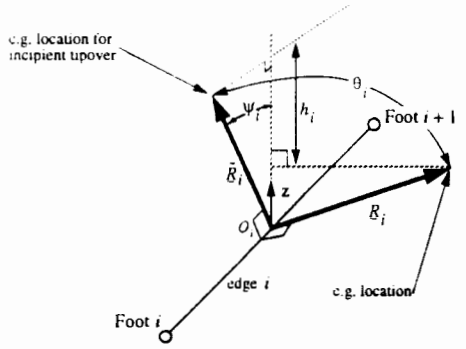

Fig. 2. Geometry for calculating the rigid stance stability measure with respect to edge i (Adapted from Messuri and Klein [1985]).

Consider a statically stable walker with $n(\geq 3)$ ground-contacting feet forming the support boundary of the walker. The rigid stance stability measure with respect to edge i, $RSSM_i$, for a given configuration of a rigid walker on rigid terrain, is the work done on the walker to move its center of gravity from an initial position (corresponding to the given configuration) to a final position where the c.g. is vertically above edge i (Fig. 2). Under the above assumptions, the work that must be done in order to tip the c.g. of the walker over an edge quasistatically is simply the change in potential energy between the initial configuration and the configuration corresponding to incipient tipover with respect to that edge. If $RSSM_i$ $(i = 1, 2, \ldots n)$ is the rigid stance stability measure of the ith edge of the support boundary (which has n edges), then the rigid stance stability measure of the walker, $RSSM_W$, is given by:

$$RSSM_W = \min\{RSSM_1, \ldots, RSSM_n\}. \qquad (1)$$

To compute the RSSM about an edge, first consider the support boundary of the walker formed by the n ground-contacting feet labeled such that foot i and foot $(i+1)$ are adjacent to each other on the support boundary. The support boundary has n edges. Edge i $(i = 1, 2, \ldots (n-1))$ is the line joining foot i and foot $(i+1)$ (Fig. 2); edge n joins foot n and foot 1.

The RSSM with respect to the ith edge is obtained by computing the work that must be done to tip the c.g. of the walker over that edge of the support boundary. For the walker c.g. to tip over the ith edge of the support boundary, its c.g. location must change by the height h_i shown in Figure 2, which is given by the following equation (Messuri and Klein 1985):

$$h_i = |\mathbf{R}_i|(1 - \cos\theta_i)\cos\Psi_i, \qquad (2)$$

where O_i is the point on edge i closest to the c.g. (see Fig. 2), $\mathbf{R}_i$ is the (initial) position vector of the c.g. relative to O_i, $\vec{\mathbf{R}}_i$ is the position vector of the c.g. relative to

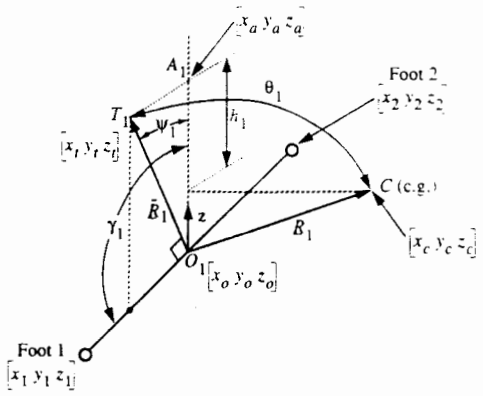

Fig. 3. Calculation of the rigid stance stability measure with respect to edge 1.

O_i when the walker has been rotated about the ith edge until the c.g. is vertically above that edge, θ_i is the angle between $\mathbf{R}_i$ and $\tilde{\mathbf{R}}_i$, and Ψ_i is the angle that $\tilde{R}_i$ makes with the vertical.

The RSSM with respect to edge i, being the change in potential energy between the initial configuration and the configuration corresponding to incipient tipover with respect to edge i, is given by

$$RSSM_i = mgh_i, \qquad (i = 1, 2, \ldots n), \tag{3}$$

where m is the mass of the walker, g is the acceleration due to gravity, and h_i is the rise in the height of the c.g. (see equation (2)). On computation of the RSSM for all edges of the support boundary, the rigid stance stability measure of the walker is obtained from equation (1).

The $RSSM_W$, as defined here, is identical to the energy stability margin (ESM) defined in Messuri and Klein (1985). A detailed procedure for computing the $RSSM_W$ is presented below. For convenience, consider tipover with respect to edge 1 of the support boundary. One must determine the change in height h_1 of the c.g. location for the walker to reach incipient tipover with respect to edge 1. The RSSM of edge 1 is then calculated from eq. (3). In lieu of using eq. (2) to compute h_1 for use in eq. (3), it is more convenient to determine h_1 as follows.

Let point O_1, $[x_o y_o z_o]^T$, denote the location on the first edge that is closest to the c.g. and let point C, $[x_c y_c z_c]^T$, denote the (known) initial location of the center of gravity of the walker. $\mathbf{R}_1$ is the position vector from O_1 to C. The vector $\tilde{\mathbf{R}}_1$ is obtained by rotating the walker about the first edge such that the c.g. location has moved to the point T_1, vertically above the first edge. Point A_1 is the projection of T_1 onto the vertical line passing through O_1. The coordinates of T_1, A_1, foot 1, and foot 2 are clearly labeled in Figure 3.

First determine the plane P that contains C and that is orthogonal to edge 1.

O_1 is then determined as the intersection of P and edge 1. The resulting equation of the plane P is

$$ax + by + cz = d, \tag{4}$$

where (x, y, z) are the Cartesian coordinates of a generic point in the plane. Defining $a = x_2 - x_1$, $b = y_2 - y_1$, and $c = z_2 - z_1$, one obtains $d = ax_c + by_c + cz_c$.

The coordinates (x, y, z) of any point on edge 1 are given by

$$\begin{aligned}[x\, y\, z]^T &= [x_1 y_1 z_1]^T + \alpha[a\, b\, c]^T \\ &= [(x_1 + \alpha a)\ (y_1 + \alpha b)\ (z_1 + \alpha c)]^T,\end{aligned} \tag{5}$$

where α is a parameter describing points on edge 1. To obtain the coordinates $[x_o y_o z_o]^T$ of the point O_1, substitute (5) into (4) to obtain the value α_o of the parameter α corresponding to point O_1:

$$\alpha_o = \frac{a(x_c - x_1) + b(y_c - y_1) + c(z_c - z_1)}{a^2 + b^2 + c^2}. \tag{6}$$

The required coordinates (x_o, y_o, z_o) of O_1 are then obtained as $x_o = x_1 + \alpha_0 a$, $y_o = y_1 + \alpha_0 b$, $z_o = z_1 + \alpha_0 c$.

The magnitudes of $\mathbf{R}_1$ and $\tilde{\mathbf{R}}_1$ are given by

$$|\mathbf{R}_1| = |\tilde{\mathbf{R}}_1| = \sqrt{(x_c - x_o)^2 + (y_c - y_o)^2 + (z_c - z_o)^2}. \tag{7}$$

The length of the line connecting foot 1 and foot 2 (edge 1) is

$$e_1 = \sqrt{(x_2 - x_1)^2 + (y_2 - y_1)^2 + (z_2 - z_1)^2}. \tag{8}$$

The angle that edge 1 makes with the vertical is given by

$$\gamma_1 = \operatorname{acos}\left(\frac{z_1 - z_2}{e_1}\right), \qquad 0 \le \gamma_1 < 180 \text{ degrees}. \tag{9}$$

The angle that $\tilde{\mathbf{R}}_1$ makes with the z-axis is given by

$$\Psi_1 = \gamma_1 - 90 \text{ degrees}, \tag{10}$$

calculation of which yields an angle between -90 and 90 degrees (Ψ_1 is positive if $z_2 - z_1 > 0$). Finally, the height of the walker c.g. location at T_1 with respect to the point O_1 may be calculated without having to determine the angle θ_1 that is required in equation (2):

$$z_t - z_o = z_a - z_o = |\mathbf{R}_1| \cos(\Psi_1). \tag{11}$$

Thus, for incipient tipover with respect to edge 1, the walker c.g. location rises by the distance

$$\begin{aligned}h_1 &= z_a - z_c \\ &= |\mathbf{R}_1| \cos(\Psi_1) + z_o - z_c.\end{aligned} \tag{12}$$

where z_r is given and z_o is determined as shown above. The rigid stance stability measure with respect to edge 1 is then given by

$$RSSM_1 = mgh_1, \tag{13}$$

where m is the mass of the walker in kilograms, g is the acceleration due to gravity, h_1 is the change in the c.g. height in meters, and $RSSM_1$ is the rigid stance stability measure over edge 1, in joules.

The rigid stance stability measure for edge i, $RSSM_i$ $(i = 1, 2, \ldots n)$ is given by

$$RSSM_i = mgh_i, \tag{14}$$

where the height h_i is determined for edge i in the same manner as shown above for edge 1.

The rigid stance stability measure of the walker is determined by first calculating the work required to tip the c.g. of the walker over each edge of the support boundary. Then, in accordance with equation (1), the rigid stance stability measure of the walker is the smallest amount of work that is necessary to tip the rigid walker over an edge of the support boundary.

4. The Compliant Stance Stability Measure

If the terrain or the legs of the walker are compliant, then it is desirable to take compliance into account in the determination of the stability of a walker. To this end, we define the compliant stance stability measure (CSSM) with respect to edge i as follows. The compliant stance stability measure, $CSSM_i$, for a given configuration of a walker with known walker/terrain compliance is the work done on the walker to move its c.g. from an initial position (corresponding to the given configuration) to a final position where the c.g. is vertically above edge i. If $CSSM_i$ $(i = 1, 2, \ldots n)$ is the work associated with tipping the c.g. over the ith edge of the support boundary quasistatically, then the compliant stance stability measure of the walker, $CSSM_W$, is given by

$$CSSM_W = \min\{CSSM_1, \ldots, CSSM_n\}. \tag{15}$$

To calculate the work required to tip the c.g. over edge i, one first ignores walker/terrain compliance and calculates the $RSSM_i$ as described in the previous section in order to determine the height that the c.g. would have to rise for the walker to tip over that edge. The combination of leg and terrain compliance will be modeled as a spring below each foot of the walker. As will be shown in the following analysis, the change in the height of the c.g. (from initial configuration to incipient tipover) as a result of placing springs below the feet is smaller than with the rigid walker–rigid terrain case of the previous section. Therefore, the change in potential energy due to the motion of the c.g. of the walker is smaller than when compliance is not taken into account. In addition, the change in potential energy of each spring must also be computed. The compliant stance stability measure for edge i is then simply the sum of the changes in potential energy of the walker and the springs. The actual computation of the $CSSM_i$ is described below. As before, the calculation is performed in the context of the walker tipping over the first edge.

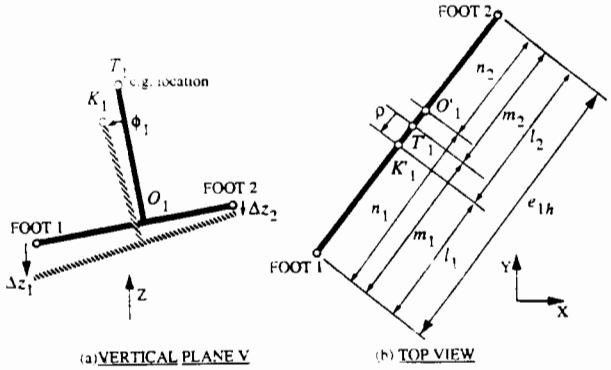

Fig. 4. Geometry of incipient tipover with respect to edge 1.

Consider the walker in a state of incipient tipover with respect to the first edge where the c.g. has moved from its original location to a point vertically above this edge (edge 1). Figure 4*A* shows the vertical plane V that contains edge 1 and the c.g. at incipient tipover. The solid and dashed lines in Figure 4*A* denote the geometry of incipient tipover before and after compliances are taken into account, respectively. T_1 and K_1 are the c.g. locations at incipient tipover before and after compliances are taken into account, respectively. The point O_1 in Figure 4*A* is the same as the point O_1 shown in Figure 3.

As shown in Figure 4*A*, the feet, in general, sink by different amounts, causing the c.g. displacement in the plane V to have both vertical and horizontal components. The horizontal component of the c.g. displacement is denoted by ρ in Figure 4*B*, which shows a top view of edge 1. In Figure 4*B*, the line joining foot 1 and foot 2 is the projection of edge 1 onto a horizontal plane; points O'_1, T'_1, and K'_1 are the projections of points O_1, T_1, and K_1 onto this plane, respectively.

The magnitudes of the horizontal distances, n_1 and n_2, between each of the two feet and the intersection point O'_1 (see Figure 4*B*) are given by

$$n_1 = \sqrt{(x_1 - x_o)^2 + (y_1 - y_o)^2}, \tag{16}$$

$$n_2 = \sqrt{(x_2 - x_o)^2 + (y_2 - y_o)^2}. \tag{17}$$

The magnitudes of the horizontal distances m_1 and m_2

between each of the two feet and the point T_1' (see Figure 4A) are given by

$$m_1 = n_1 - |\mathbf{R}_1| \sin(\Psi_1), \tag{18}$$

$$m_2 = n_2 + |\mathbf{R}_1| \sin(\Psi_1). \tag{19}$$

where $|\mathbf{R}_1|$ and Ψ_1 are given by eq. (7) and eq. (10), respectively. The magnitude of the horizontal distance between the two feet is given by

$$e_{1h} = \sqrt{(x_2 - x_1)^2 + (y_2 - y_1)^2}. \tag{20}$$

Note that from the geometry of Figure 4, $e_{1h} = l_1 + l_2 = m_1 + m_2 = n_1 + n_2$.

Let the (positive) magnitudes of vertical forces exerted on foot 1 and foot 2 by the terrain when the walker is in its given original stance be denoted by f_1 and f_2, respectively. In general, since other feet are also in ground contact, $(f_1 + f_2)$ is less than the weight W of the robot. However, at incipient tipover with respect to edge 1, the total weight of the walker is supported by foot 1 and foot 2, and the tilt in the vertical plane V due to compliance causes the walker c.g. to shift from point T_1 to point K_1. If l_1 and l_2 are the horizontal distances between each foot and the new c.g. location, as shown in Figure 4B, and if the magnitudes of new vertical foot forces on foot 1 and foot 2 at incipient tipover, are $\tilde{f}_1$ and $\tilde{f}_2$, respectively, then the following four relationships between these four variables ($l_1, l_2, \tilde{f}_1$, and $\tilde{f}_2$) apply:

$$\tilde{f}_1 + \tilde{f}_2 = W, \tag{21}$$

$$l_1 \tilde{f}_1 \cong l_2 \tilde{f}_2, \tag{22}$$

$$l_1 + l_2 = e_{1h}, \tag{23}$$

$$l_2 + \eta_1 \tilde{f}_1 + \eta_2 \tilde{f}_2 = \Lambda, \tag{24}$$

where

$$\eta_1 = \frac{|\mathbf{R}_1| \cos^2 \Psi_1}{k_1 e_1}, \tag{25}$$

$$\eta_2 = -\frac{|\mathbf{R}_1| \cos^2 \Psi_1}{k_2 e_1}. \tag{26}$$

and

$$\Lambda = m_2 + \left(\frac{|\mathbf{R}_1| \cos^2 \Psi_1}{k_1 k_2 e_1} \right) (k_1 f_2 - k_2 f_1). \tag{27}$$

Equation (22) is based on ignoring the moments due to the horizontal components of the contact forces. However, these moments, and moments exerted by the terrain on (large) feet, can be incorporated in the statistical analysis. Equation (24) was obtained as follows. The distance ρ, shown in Figure 4, is the horizontal displacement of the c.g. due to the vertical deflections of the feet constituting the edge at which tipover is incipient. From the geometry of Figure 4, ρ is given by the following equation:

$$\rho = 2|\tilde{\mathbf{R}}_1| \sin\left(\frac{\phi_1}{2}\right) \cos\left(\Psi_1 + \frac{\phi_1}{2}\right). \tag{28}$$

For small foot deflections, the angle ϕ_1 is related to the walker geometry by

$$\tan(\phi_1) \cong \frac{(\Delta z_2 - \Delta z_1)\cos(\Psi_1)}{e_1}. \tag{29}$$

where Δz_1 and Δz_2 are the displacements of the springs under foot 1 and foot 2, respectively (see Figure 4A).

If the displacements of these feet are small, then ϕ_1 is small and equation (28) simplifies to:

$$\rho = \frac{|\mathbf{R}_1|(\Delta z_2 - \Delta z_1)}{e_1} \cos^2 \Psi_1, \tag{30}$$

where e_1 is determined from equation (8).

The vertical foot displacements (sinkages) may be found from the spring (walker/terrain) compliances and the changes in forces on the two feet of the edge over which tipover takes place. If the soil under the feet is consolidated, as in most cases, it is reasonable to assume a linear terrain compliance (Nagy 1991). The vertical displacements Δz_1 and Δz_2 are then

$$\Delta z_1 = \frac{-(\tilde{f}_1 - f_1)}{k_1} \tag{31}$$

and

$$\Delta z_2 = \frac{-(\tilde{f}_2 - f_2)}{k_2}, \tag{32}$$

where k_1 and k_2 are the vertical effective stiffnesses of the combination of the leg and the terrain under foot 1 and foot 2, respectively. The variables ρ, l_2, and m_2 are related by

$$\rho = l_2 - m_2. \tag{33}$$

Equation (24) was then obtained by substituting (31)–(33) into (30).

Equations (21)–(24) form a set of four equations that can be solved for l_1, l_2, $\tilde{f}_1$, and $\tilde{f}_2$. Of these equations, three are linear, and one (equation (22)) is a simple, nonlinear equation. From these equations the value of the variable l_1 is obtained as follows:

$$l_1 = e_{1h} \left(\frac{e_{1h} + \eta_1 W - \Lambda}{e_{1h} + (\eta_1 - \eta_2) W} \right). \tag{34}$$

The next step is to obtain l_2 from equation (23):

$$l_2 = e_{1h} - l_1. \tag{35}$$

Now $\tilde{f}_2$ can be obtained from equations (21) and (22) as

$$\tilde{f}_2 = \frac{l_1 W}{e_{1h}}. \tag{36}$$

Finally, $\tilde{f}_1$ is obtained from equation (21) as

$$\tilde{f}_1 = W - \tilde{f}_2. \tag{37}$$

The force magnitudes $\tilde{f}_1$ and $\tilde{f}_2$ are substituted into equations (31) and (32) in order to determine the foot sinkages Δz_1 and Δz_2. Finally, the height that the walker's c.g. must rise relative to its original position is determined by

$$h_{c1} = h_1 - 2|\mathbf{R}_1| \sin\left(\frac{\phi_1}{2}\right) \sin\left(\Psi + \frac{\phi_1}{2}\right) + \Delta z, \tag{38}$$

where ϕ_1 is determined from equation (29),

$$\Delta z = \Delta z_2 - \frac{n_2}{e_{1h}}(\Delta z_2 - \Delta z_1), \tag{39}$$

and h_1 is the change in c.g. height, as given by equation (12), for incipient tipover with respect to edge 1 if there was no walker/terrain compliance. The change in spring energies are also required to determine the work that must be done on the walker to achieve incipient tipover. The springs of the two legs that constitute the edge over which tipover is incipient are further compressed; the remaining legs uncompress their springs (and eventually separate from them). If $\delta_j = f_j/k_j$, $(\delta_j \geq 0)$, is the initial compression of the spring under leg j before the tipover process begins, and $\tilde{\delta}_j = \tilde{f}_j/k_j$ is its final compression (zero for all feet other than the two constituting the edge over which tipover is incipient), then the change in potential energy of spring j, ΔE_{spr_j}, due to the tipover process is given by

$$\Delta E_{\text{spr}_j} = \frac{1}{2} k_j \left(\tilde{\delta}_j^2 - \delta_j^2\right). \tag{40}$$

Thus the compliant stance stability measure for edge 1 is

$$CSSM_1 = mgh_{c1} + \sum_{j=1}^{n} E_{\text{spr}_j}, \tag{41}$$

where m is the mass of the walker in kilograms, g is the acceleration due to gravity in m/s^2, h_{c1} is the change in the c.g. height in meters, and $CSSM_1$ is the compliant stance stability measure of edge 1, in joules.

The compliant stance stability measure for edge i, $CSSM_i$, $(i = 1, 2, \ldots n)$, is computed in exactly the same manner as for edge 1. The $CSSM_i$ is therefore given by

$$CSSM_i = mgh_{ci} + \sum_{j=1}^{n} E_{\text{spr}_j}, \qquad (i = 1, 2, \ldots n). \tag{42}$$

The compliant stance stability measure of the walker is determined by first calculating the work (i.e., the change in potential energy) required to tip the walker over each edge of the support boundary. Then, in accordance with equation (15), the compliant stance stability measure of the walker is the smallest amount of work required to tip the walker over an edge of the support boundary.

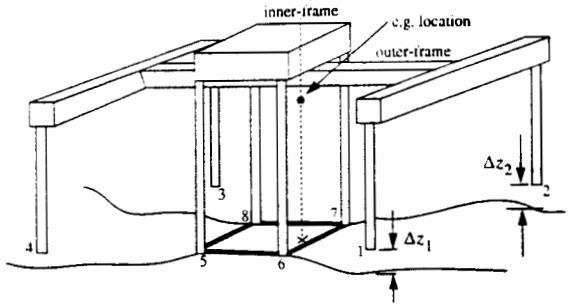

Fig. 5. A robot configuration where the $RWSM_W$ is larger than the $RSSM_W$.

5. Walker Stability Measures

The stability measures discussed so far take only the ground-contacting feet into account in quantifying the stability of the walker. However, there are a number of walking machines for which feet that are not in ground contact improve the walker's ability to resist tipover. For example, in Hirose (1989) the "stability" of a quadruped trot can alternate between static and "dynamic." The latter case corresponds to allowing the walker to stand on two legs during a limited portion of the gait cycle based on the knowledge that the remaining two (non–ground-contacting) legs will resist the possible falling of the walker. We will next analyze the effect of non–ground-contacting legs on static stability. This leads to the definition of walker stability measures that, by more completely taking walker geometry into account, address the actual falling of the walker.

Consider the frame walker, shown in Figure 5, that consists of two frames that may be moved relative to each other. Each frame has four legs that can translate in the vertical direction (for a level machine). The walker moves by placing the feet of one of the frames firmly on the terrain and raising the feet of the other frame. The latter frame may now be moved (by an appropriate translation and rotation) with respect to the frame whose feet contact the ground. In the figure shown, the walker is resting on its inner frame (comprising feet 5–8), while the outer frame (comprising feet 1–4) is free to move relative to the ground. The traditional interpretation of walker stability predicts that the machine is close to falling over when the projection of the walker's c.g. onto a horizontal plane is near the support polygon formed by the ground-contacting feet (feet 5–8).

Consider the case (shown in Figure 5) where the walker tips over the edge that connects foot 6 to foot 7. If foot 1 and foot 2 are sufficiently close to the ground, as shown in Figure 5, then these feet may stop the walker from falling over when the c.g. tips over the edge formed by foot 6 and foot 7. If the walker tips over the edge of the support boundary formed by foot 6 and foot 7, then foot 1 and foot 2 drop by the amounts Δz_1 and Δz_2, respectively (see Fig. 5). The walker would now have to tip over the new edge formed by the newly ground-contacting feet (feet 1 and 2) if it is to fall over in the same direction. The net work required to cause the walker to fall will clearly be greater than the work computed by the RSSM or CSSM with the original support boundary. We therefore define two new stability measures for which the configuration and the type of walker are more completely taken into account. The rigid walker stability measure (RWSM) and the compliant walker stability measure (CWSM) are the walker stability counterparts of the RSSM and CSSM, respectively. The walker stability measures are calculated in a similar manner to their stance stability counterparts; therefore, only an outline of the method for calculating these measures is presented in this section, with appropriate references to the previous sections for relevant details.

The stance stability measures only consider the stabilizing effects of those ground-contacting feet that form the support boundary. We will henceforth designate the original support polygon and the original support boundary as the *inner support polygon* and the *inner support boundary* (ISB), respectively. In contrast to the stance stability measures, the walker stability measures also consider the stabilizing effects of those feet that are close to (but not in contact with) the terrain. Such feet are said to be in "terrain-following mode," and the height of a terrain-following foot above the ground is called its *terrain-following height*. The *outer support polygon* is defined as the convex hull of the projections onto a horizontal plane of all feet that are either in ground contact or in the terrain-following mode. The *outer support boundary* (OSB) is the boundary formed by the line segments connecting those adjacent feet whose projections comprise the outer support polygon. For example, the outer support polygon and boundary of the walker depicted in Figure 5 is formed by feet 1–4. Figure 6 depicts the inner and outer support polygons for the frame walker configuration shown in Figure 5.

From the above discussion, it is clear that for the case of robots like this frame walker, there are two destabilizing failure modes that must be considered: stance instability and walker instability. A systematic procedure for determining the corresponding stance stability and walker stability measures is depicted in Figure 7 and discussed below.

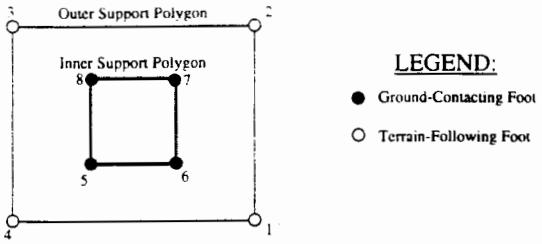

Fig. 6. The inner and outer support polygons for the frame walker.

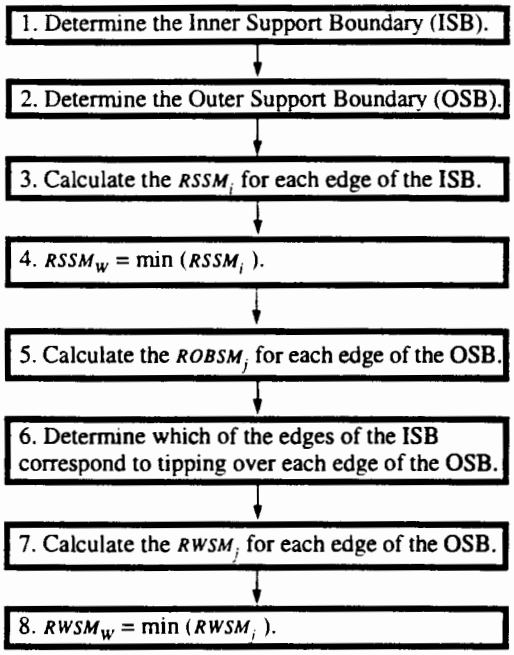

Fig. 7. Procedure to calculate the rigid walker stability measure.

To calculate the rigid walker stability measure of a walker (the $RWSM_W$), first the inner and outer support boundaries are determined. Then the rigid stance stability measure $RSSM_i$ for each edge of the inner support boundary of the walker is calculated as described in Section 3. This is done by calculating the energy associated with tipping the walker over each edge of that boundary. Recall that the $RSSM_i$ calculates the minimum amount of work to tip the c.g. of the walker over edge i, assuming that feet that are not in ground contact have no effect on the stability of the walker. However, if there are non–ground-contacting feet that could constrain a fall, much more work may be required to tip the walker over an edge of the inner support boundary than that calculated by the RSSM.

To determine the rigid walker stability measure, the work required to tip the c.g. over each edge of the outer support boundary, the $RWSM_j$ must be determined. Tipping the c.g. of the walker over an edge of the outer

support boundary involves, in general, first tipping the c.g. over an edge of the inner support boundary. This results in a change in the stance of the walker. The method of calculating the $RWSM_j$ is to first "ignore" the effects of the inner support edges in calculating the work to tip over an outer support boundary edge; this work will be called the *rigid outer boundary stability measure*, $ROBSM_j$, for edge j of the OSB. If two adjacent feet of edge j on the outer boundary are in ground contact, then this edge is also an edge of the inner support boundary, and therefore, the outer boundary stability measure with respect to that edge, $ROBSM_j$, is exactly the same as the corresponding stance stability measure ($RSSM_j$) for that edge. For edges that have one or both feet that are not in ground contact, when tipping over that edge, these feet drop into contact with the terrain surface. The corresponding change in mechanism geometry may be approximated by assuming that the terrain-following feet of the edge being considered drop vertically until they make ground contact, since they are, by definition, close to the ground. The change in height h of the c.g. in order to tip the walker over an edge of the outer support boundary is determined as follows. First compute the rise r in height of the c.g. when the walker is rotated about the line joining the actual positions of the two feet (which constitute the edge under consideration) from its original configuration until incipient tipover is reached (with respect to the edge). Next compute the drop d in the height of the c.g. when the two feet drop vertically until they make ground contact. The required change in height, $h = r - d$. The drop d is computed in the same manner as the drop in c.g. location due to spring deflections (see Section 4 and Figure 4).

Now, for each edge of the outer support boundary, determine all possible edges of the inner support boundary over which the c.g. must cross in order to tip the c.g. over that edge. For example, consider the frame walker of Figure 5 in the configuration shown in plan view in Figure 8. The possible ISB edges over which the c.g. must travel in order to tip over each edge of the OSB is given in the table that is part of Figure 8. If the work required to tip the c.g. over all of these inner support boundary edges is greater than the rigid outer support boundary measure, the $ROBSM_j$, then that outer boundary edge does not contribute to the stability of the walker.

Having determined which edges of the inner support boundary correspond to tipping over each edge of the outer support boundary, the rigid walker stability measure, $RWSM_j$, may be calculated for each edge j of the outer support boundary. If the minimum of the $RSSM_m$ of the edges of the inner boundary that correspond to tipping over the outer edge j is greater than the $ROBSM_j$, then the $RWSM_j$ is equal to this minimum. Otherwise, the $RWSM_j$ is equal to the $ROBSM_j$. Thus, the rigid

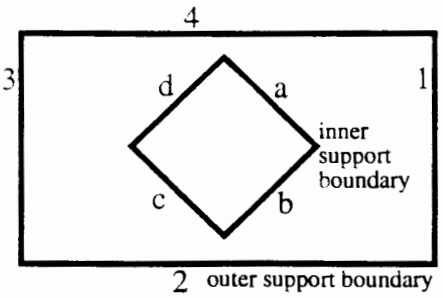

OSB	ISB
1	a , b
2	b , c
3	c , d
4	a , d

Fig. 8. Determination of the edges of the ISB that correspond to tipping over each edge of the OSB.

walker stability measure of edge j is

$$RWSM_j = \max\{ROBSM_j, \min(RSSM_1, \ldots, RSSM_M)\}. \quad (43)$$

The rigid walker stability measure of the walker, $RWSM_W$, is the minimum value of the $RWSM_j$ of all edges of the outer support boundary; i.e.,

$$RWSM_W = \min\{RWSM_1, \ldots, RWSM_p\}, \quad (44)$$

where p is the number of edges of the outer support boundary.

We have shown how to calculate the rigid walker stability measure of a walker. The procedure to calculate the compliant walker stability measure is the same as that shown in Figure 7, except that one additionally takes the walker/terrain compliance into account in the manner described in Section 4.

From equations (44), (43), and (1) it is clear that

$$RWSM_W \geq RSSM_W. \quad (45)$$

In a similar fashion, one can show that

$$CWSM_W \geq CSSM_W. \quad (46)$$

The walker stability measure equals the corresponding stance stability measure when all feet are in ground contact, or when feet that are not in ground contact are so far above the ground that they do not affect the stability of the walker with respect to tipping and falling over an edge.

6. Applications

In this section, a comparison will be made between the various stability measures developed in this work. In Section 6.1, the rigid stance stability measure $RSSM_W$ will be compared to the compliant stance stability measure $CSSM_W$ for a walker that has all its feet in contact with compliant terrain. Then the $RSSM_W$ will be compared

to the rigid walker stability measure $RWSM_W$ for a rigid frame walker on rigid terrain where the initial stance of the walker is such that the feet of the outer frame are not in ground contact. In Section 6.2, the choice of the appropriate stability measure based on walker type, walker stance, and terrain compliance is discussed. The use of stability measures in the type selection of walkers, gait planning, and walking control is then discussed in Section 6.3.

6.1. *Comparison of Stability Measures*

Example 1: The AMBLER

The AMBLER is a six-legged walking robot developed at Carnegie Mellon University for planetary exploration. A plan view of the geometry of this walker is shown in Figure 9. The body of the walker is represented by a horizontal line, and the walker is shown in an initial and final configuration corresponding to a 1-meter propulsion of the walker in the Y direction with the locations of all feet fixed. The $RSSM_W$ and $CSSM_W$ measures for this propulsion example are shown in Figures 10 and 11 for the case of the walker on flat and sloped sandy terrain, respectively. In the former case, the $CSSM_W$ is essentially equal to the $RSSM_W$ throughout the walker motion. With the walker on a 30-degree slope of sand, the $CSSM_W$ is approximately 5% to 10% less than the $RSSM_W$. The reason for the greater difference between the two stability measures in the case of the sloped terrain is that the sloped terrain contacts have greater effective vertical compliance (Manko 1990). (The walker/terrain stiffness for these two examples were obtained from experimental data [Manko 1990].)

It is possible to have a significant difference between the $RSSM_W$ and $CSSM_W$ even when the walker is on flat terrain. The $RSSM_W$ and $CSSM_W$ measures are shown for different values of terrain stiffness in Figure 12. For clarity, the different values of stiffness in Figure 12 have been normalized with respect to the stiffness $K(= 307.6\,\text{kN/m})$ that was used in the flat terrain

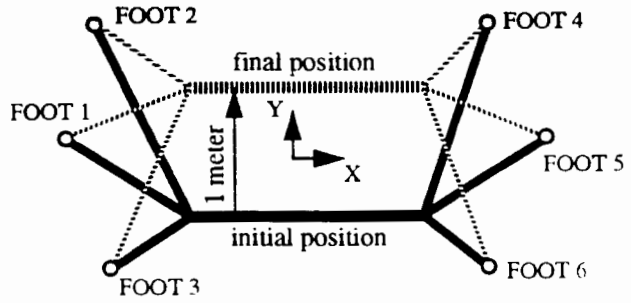

Fig. 9. Plan view of the initial and final position of the AMBLER.

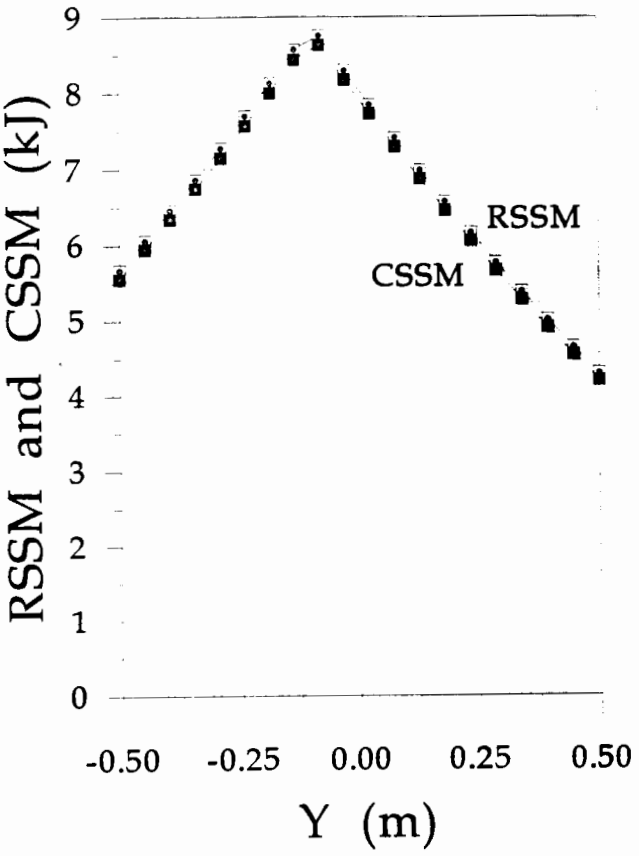

Fig. 10. Comparison of the $RSSM_W$ and $CSSM_W$ for forward propulsion of the AMBLER on flat terrain.

example depicted in Figure 10. This clearly shows that if the $RSSM_W$ (i.e., the ESM of Messuri and Klein [1985]) is used for a walker that is on very compliant terrain, the stability measure of that walker is overestimated. If an overestimate of a stability measure of the walker is used as a basis for planning a walker motion, then the execution of this planned motion might jeopardize the stability of the walker. To avoid such a situation, the appropriate compliant stability measure should be used as a basis for evaluating planned walker motions.

Example 2: The Frame Walker

The $RSSM_W$ and $RWSM_W$ for propelling a frame walker of size and mass comparable to the AMBLER is now considered. In this example, the outer frame is propelled 1 m in the Y direction as shown in Figure 13. Only the feet of legs 1 through 4 (the inner frame) are in ground contact; the other feet, which belong to the outer frame, are located 20 cm above ground level throughout the trajectory. Throughout the trajectory, the inner support boundary comprises feet 1 through 4, and the outer support boundary comprises feet 5 through 8. The inner

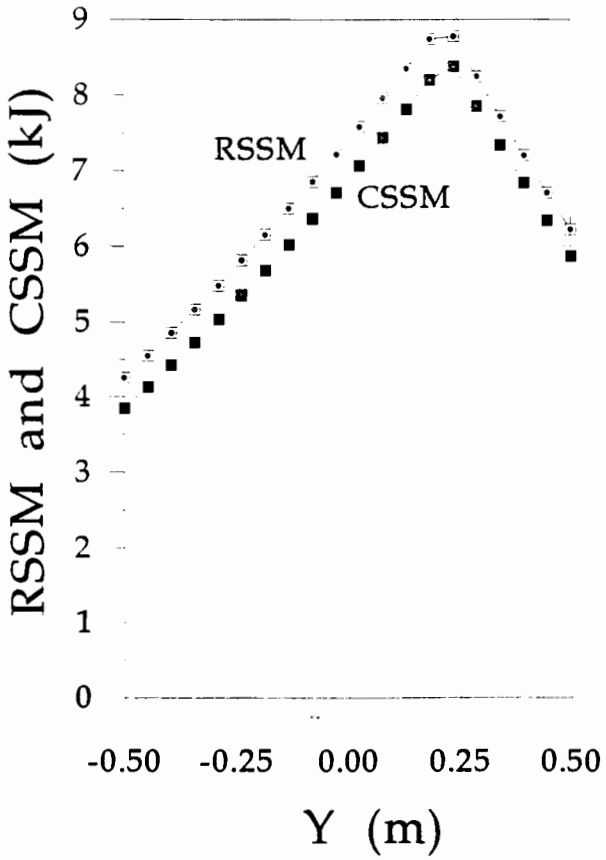

Fig. 11. The $RSSM_W$ and $CSSM_W$ for simulated propulsion of the AMBLER on a slope.

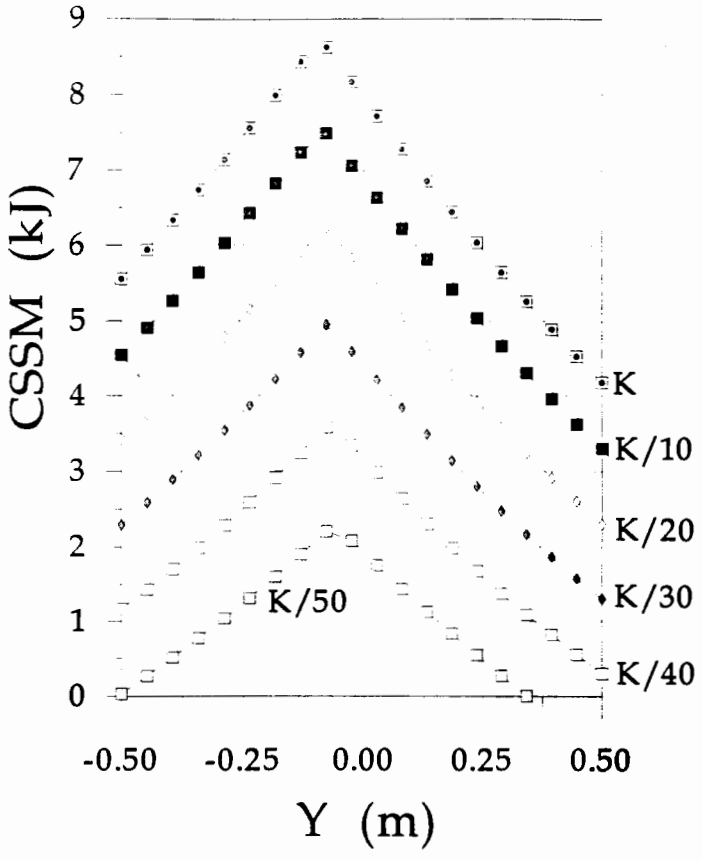

Fig. 12. The $RSSM_W$ and $CSSM_W$ for differing terrain stiffness (AMBLER propulsion on flat terrain).

and outer frames are square frames with sides of 2 m and 5 m, respectively. The walker is on flat, rigid ground and, as with the AMBLER propulsion example, its c.g. is located about 3.9 m above the flat ground surface. The $RWSM_W$ values corresponding to this trajectory for different terrain-following heights (the height of each of feet 5 through 8 above the terrain) are shown in Figure 14. Also shown in this figure is the $RSSM_W$ for the trajectory. Note that for a terrain-following height $\geq$ 100 cm, $RWSM_W = RSSM_W$—i.e., the outer frame does not improve the stability of the walker for this "move".

Ideally, to maximize walker stability, the terrain-following height of the feet not in ground contact should, in the limit, approach zero; this limiting case is included in Figure 14 to show the upper bound on the tipover stability of this walker. From the results shown in Figure 14, it is clearly desirable for the terrain-following feet to be as close to the terrain as possible when moving the outer frame. If the terrain-following feet are too far above the surface, (about 100 cm in this example), they will not improve the tipover stability of the walker.

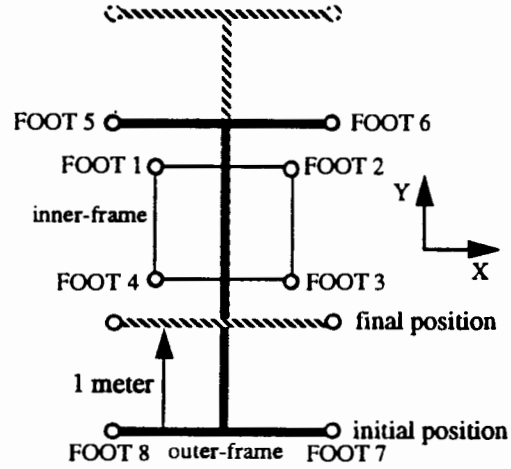

Fig. 13. Plan view of the initial and final position of the frame walker.

The terrain-following height has no effect on walker stability when the walker rests on the outer frame, and the feet of the inner frame are not in ground contact. In this instance, the stability of the walker is governed only by the relative locations of the feet of the outer frame.

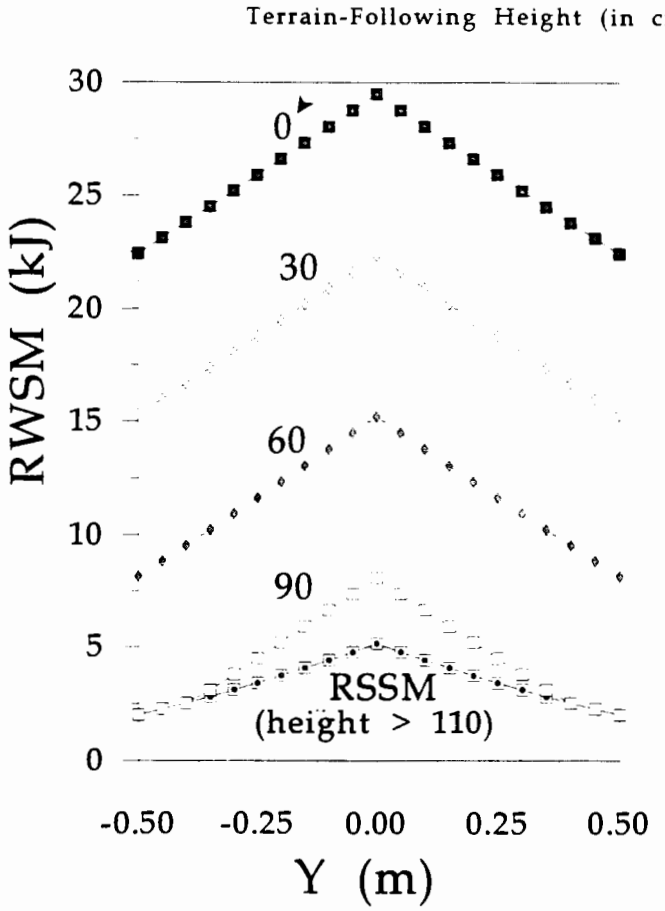

Fig. 14. Comparison of the $RSSM_W$ and $RWSM_W$ for the frame walker for different terrain-following heights.

6.2. Selection of Stability Measures

To determine the appropriate stability measure for use in a given context, proceed as follows:

1. Decide whether the combination of the walker and terrain is rigid or compliant.
2. Determine the inner and outer support polygon for the given configuration of the walker (see Section 5).
3. Determine whether the inner and outer support polygons are identical to or different from each other.
4. Use the decisions made in steps 1 and 3 in conjunction with the stability measure selection matrix shown in Figure 15 to select the appropriate stability measure.

Using the above procedure, the characteristics of the mechanism and terrain are then combined to determine whether the $RSSM_W$, $CSSM_W$, $RWSM_W$, or $CWSM_W$ should be used for planning walker motions and for monitoring the stability of the walker as it executes these motions. For example, consider the case of

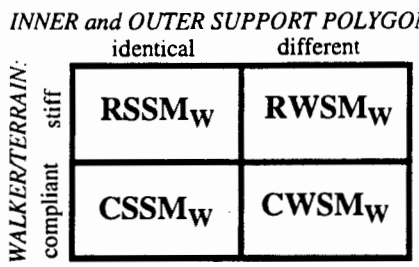

Fig. 15. Stability measure selection matrix.

the AMBLER when it walks in its laboratory testbed. The terrain of the testbed is very stiff, as it has a relatively thin layer of sand on a concrete floor. Furthermore, the AMBLER moves by picking up only one leg at a time (at least five feet remain in ground contact at any time); consequently, the inner support polygon and outer support polygons are either exactly the same, or nearly the same, at all times. According to the stability measure selection matrix of Figure 15, the appropriate measure for this case is the $RSSM_W$. For the case of the frame walker on rigid terrain, because the inner and outer support polygons can be quite different, the $RWSM_W$ should be used to "measure" stability.

As discussed in Example 1 of Section 6.1, the compliant stability measures should be used for assessing the stability of walkers that are compliant, or on compliant terrain. To be able to use such measures, the vertical leg–terrain compliance for each ground-contacting foot must be estimated. The compliance of new footfalls may be determined by measuring the change in vertical foot force, and the corresponding vertical displacement of the foot making (new) ground contact.

6.3. The Use of Stability Measures

6.3.1. Type Selection of Walkers

If reliable locomotion is a primary concern, then stability measures should also be used to aid in the selection and evaluation of an appropriate walker type from a set of candidate walker designs. To illustrate this, we will discuss how stability measures were used to evaluate two proposed designs for a new CMU walking robot to explore an active volcano (Mount Erebus) in Antarctica. These two designs—the rectangular-frame walker and the parallelogram-frame walker—are shown (in plan view) in Figure 16.

Both walker designs consist of eight legs; each walker has two frames of four legs each. There is a rotational degree of freedom between the two frames to allow rotation of one frame with respect to the other. Propulsion is achieved by a motor on each frame that moves the four

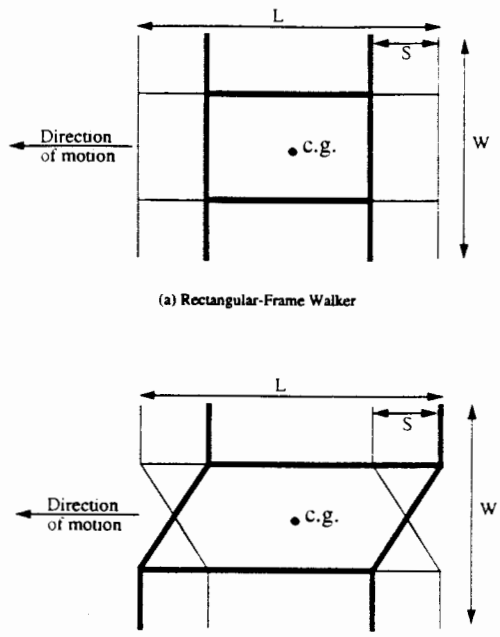

Fig. 16. Plan view of two competing robot designs for the Erebus Project.

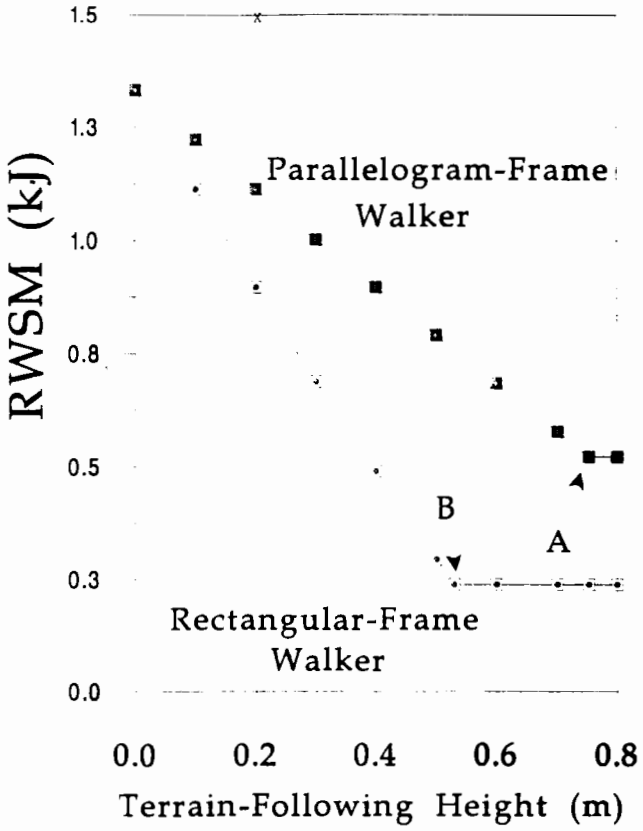

Fig. 17. Walker stability of the two designs for different terrain-following heights.

legs on that frame in unison through a four-bar linkage at each leg. For each walker schematic shown in Figure 16, the thick lines represent one frame, and the thin lines represent the other frame. For the geometry and aspect ratio shown (W = 2.25 m, L = 2.5 m, and height = 1.5 m), the stance stability of the parallelogram-frame walker is relatively insensitive to its configuration, while the stance stability of the rectangular-frame walker varies significantly as the walker switches its stance from the inner frame to the outer frame or vice versa. When the feet of the outer frame of the rectangular-frame walker are in ground contact, then the rectangular-frame walker has much higher stance stability than the parallelogram walker (when the latter walker is standing on any one of its two frames). Conversely, when only the feet of the inner frame of the rectangular-frame walker are in ground contact, then the rectangular-frame walker has significantly lower stance stability than the parallelogram-frame walker.

From a design standpoint, one would like to compare the stability of the walkers for the "worst-case" stance when the stability of each walker is a minimum. From a stance stability perspective, the parallelogram-frame walker is preferable to the rectangular-frame walker. However, from a mechanical design perspective, the rectangular-frame walker is preferable, as the drivetrains that distribute the propulsion power are considerably lighter and less complex for the rectangular-frame design. Bearing in mind that walker stability is a more effective measure than stance stability of the resistance to tipover (which is the primary concern), we quantify the former for the two competing designs in an attempt to resolve the apparent design conflict between simplicity and stability.

The $RWSM_W$ for the two designs is shown in Figure 17; in each case the walker mass is 300 kg. The $RWSM_W$ is computed for the "worst" case—i.e., the walker configuration that is least stable. The least stable configuration occurs when the walker stands on the inner frame with all legs of that frame drawn back with respect to the direction of walker motion. In Figure 17, the $RWSM_W$ of each walker is plotted as a function of terrain-following height. When the terrain-following height is very large, the feet that are not in ground contact do not contribute to walker stability, and the $RWSM_W$ for the parallelogram-frame walker is significantly higher than that of the rectangular-frame walker. In the limiting case—points A and B in Figure 17—the $RWSM_W$ approaches the $RSSM_W$ for each walker. Therefore, as stated earlier, the use of the $RSSM_W$ as a basis for evaluation of the two designs would strongly favor the parallelogram-frame walker. (It is worth noting that the minimum terrain-following height at which a foot no longer contributes to the stability of the parallelogram-

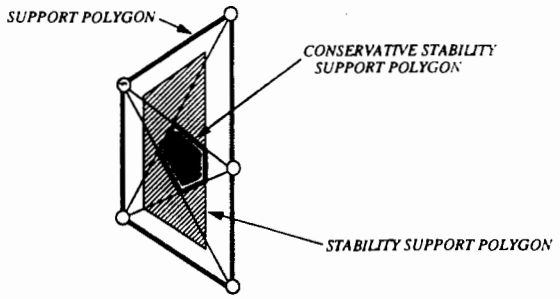

Fig. 18. The conservative stability support polygon.

frame walker (point A in Figure 17) is greater than the corresponding height (point B) for the rectangular-frame walker owing to the differing walker geometries.) However, if the terrain-following height is small (< 20 cm), then the magnitudes of the $RWSM_W$ for the two walkers are sufficiently close, implying that from a stability standpoint, the two designs are both acceptable. Because, as mentioned previously, the rectangular-frame walker has the advantage of a simple mechanical design, and, for small terrain-following heights, its walker stability measure is close enough to that of the parallelogram-frame walker, the rectangular-frame walker design type is preferable to the parallelogram-frame walker. The rectangular-frame walker was indeed the walker type selected for the Erebus mobile robot design.

6.3.2. Gait Planning

To achieve reliable locomotion, a planned walker gait must, at the very least, maintain a specified minimum level of the appropriately selected stability measure. The use of stability measures to evaluate and plan reliable gaits will now be discussed.

The region of the support polygon above which the c.g. of the walker must lie in order to satisfy the minimum stability requirement must first be determined. For a given walker c.g. height, the locus of all points in a horizontal plane for which the appropriate stability measure has constant magnitude is a polygon, each edge of which corresponds to an edge of the support polygon. If the magnitude of the stability measure for the boundary of the polygon is the minimum allowable level for that measure, then the polygon corresponding to this minimum threshold is called the *stability support polygon* (SSP) (Fig. 18). All points within the stability support polygon correspond to c.g. locations that exceed the minimum stability threshold.

The first step in gait planning is to select the appropriate stability measure for the walker configuration and walker/terrain compliances using the stability selection matrix in Section 6.2. Then one decides on an allowable minimum threshold for the selected stability measure: gaits should be planned such that the stability measure of the planned walker motion is always greater than the specified threshold. For a given c.g. height, determine the stability support polygon corresponding to the chosen threshold. If the walker's c.g. height varies during the planned motion, then a stability support polygon is defined for several different levels of c.g. height. If the gait planner is constrained to generate a walker motion that keeps the projection of the c.g. inside the stability support polygon, then the planned motion is reliable (i.e., safe).

To further enhance the stability and reliability of locomotion, one could further constrain the walker c.g. location to lie above both the conservative support polygon and the stability support polygon. Recall from Section 1.1 (Fig. 1) that the conservative support polygon, CSP, is defined as the region above which the c.g. must be located such that the support failure of any one leg does not destabilize the machine. However, one drawback of using only the CSP for motion planning arises if there are three collinear feet in the support polygon out of a total of five ground-contacting feet, as shown in Figure 1. For this case, the CSP touches the middle foot of the three (at the edge of the support polygon), thereby allowing some planned motions in which the c.g. position approaches incipient tipover! For those applications where stability is of utmost concern, the conservative support polygon could be intersected with the stability support polygon, yielding the *conservative stability support polygon* (CSSP) shown in Figure 18. Typically, the CSSP is too conservative for most applications; if used in motion planning, the CSSP constraint yields high stability at the expense of reduced walking speed. As a consequence, the CSSP should only be used if the speed of the walking is of no concern; otherwise, the SSP should be used in the planning of walker motions.

The constraints placed on gait planning by stability requirements for the walker may be augmented by other constraints on the walker–terrain interaction in order to ensure reliable locomotion. For example, if the planned walker motions lead to an undesirable foot force distribution, the move should not be allowed, even if it satisfies the stability constraint (Nagy, Desa, and Whittaker 1992).

6.3.3. Control

To ensure reliable locomotion, the controller of a walking robot should monitor the appropriate stability measure online. Comparison of the actual stability measure with its predicted value may be used to detect anomalous interaction between the walker and terrain.

The method for how to use stability analysis in real-time control is as follows. First, the stability selection matrix of Section 6.2 should be used to choose the appropriate stability measure, depending on the type of

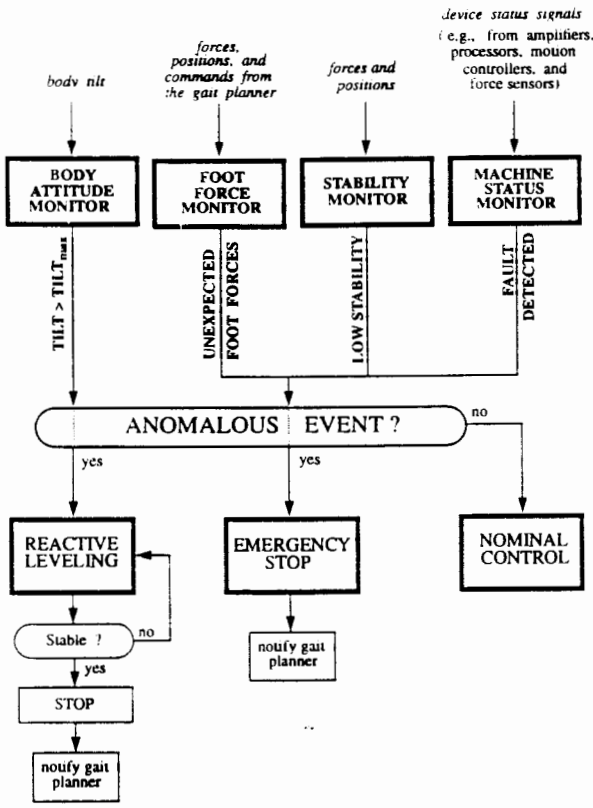

Fig. 19. A controller architecture for statically stable, walking robots.

walker and the terrain. During gait planning, the values of the stability measure of the walker during a planned walker motion are predicted. When the planned motion is executed, the actual value of the stability measure of the walker is calculated in real time. The actual stability measure is compared with the predicted stability measure throughout the walker trajectory. The walker–terrain interaction is favorable (and the desired stability level is achieved) when the predicted and actual stability measures are close in some specified sense and, additionally, the actual stability measure is above some threshold. If the predicted and actual stability measures are not close, then reactive control measures should be taken to safeguard the robot.

As an example of how stability monitoring should be used in the real-time control of a statically stable walking robot, consider the context of controlling the AMBLER. The prescription for walking shown in Figure 19 and described in Nagy, Whittaker, and Desa (1992) consists of nominal control, as well as reactive control measures. If an anomalous situation arises, such as support failures that start to tip the walker over, poor stability, unusual foot forces, or component failure, then nominal control is interrupted, and the appropriate reactive measure is taken.

As discussed in Section 6.1, the appropriate stability measure for the AMBLER on compliant terrain is the compliant stance stability measure, or $CSSM_W$. For the AMBLER on such terrain, the $CSSM_W$ should be calculated in real time and compared with the predicted value throughout the walker motion. If the magnitude of the actual $CSSM_W$ for a motion is above the minimum allowable threshold and the following condition,

$$\left| \frac{(CSSM_W)_{\text{actual}} - (CSSM_W)_{\text{predicted}}}{(CSSM_W)_{\text{predicted}}} \right| \leq \alpha, \qquad (47)$$

where α is a predetermined bound on stability error, is satisfied, then the actual motion is considered safe. If condition (47) is violated or the magnitude of the actual $CSSM_W$ is below the allowable threshold for the gait, then an appropriate reactive control action should be taken. With slowly moving, multilegged walkers such as the AMBLER, the reactive control action is simply to halt the robot and then establish a new stable stance. However, low stability might arise from the walker starting to tip over (which may be sensed from inclinometers or angular rate sensors), in which case reactive leveling is used to ensure the safety of the robot (Nagy, Wu, and Dowling 1991).

In general, the measure used, the bound on stability measure, and the appropriate reactive response to low estimated (actual) walker stability is robot and application dependent. For example, the walker stability measures should definitely be used with the frame walker type of robot, although the corresponding stance stability measures may be used in addition, if appropriate. The best method for determining the bound α in equation (47) is through experiments on the walker to which it is applied; the bound should not be so small that it continually interrupts walking for no apparently good reason. In lieu of immediately stopping the walker when the actual value of the stability measure is below the threshold, other possible reactive control actions are to bring non–ground-contacting feet into ground contact, and/or extending the legs corresponding to the support edge over which the walker is most likely to tip.

7. Summary and Conclusions

This work has shown that it is important to differentiate between stance stability and walker stability. Stance stability refers to the ability of a walker to maintain a given stance in the presence of disturbances, while walker stability refers to the ability of a walker to avoid tipover in the presence of disturbances. It is also important to take the compliance of the terrain and the walker into account in the determination of stability. The two types of stability and compliance were combined with the idea of the

energy stability margin (Messuri and Klein 1985) to systematically yield the four stability measures developed in this work—namely, the rigid stance stability measure, the compliant stance stability measure, the rigid walker stability measure, and the compliant walker stability measure. These stability measures were then applied to a variety of situations in order to demonstrate their proper use.

Terrain compliance can significantly affect the magnitude of a stability measure. In Section 6.1, it was demonstrated that not taking terrain (and walker) compliance into account may result in a significant overestimate of the stability of the walker. As a result, walker motions that are planned based on these erroneous estimates may not be dependable. Therefore, for a compliant walker or compliant terrain, it is necessary to take compliance into account when measuring the stability of that walker. It was also shown that walkers whose inner and outer support polygons are significantly different (see Example 2 in Section 6.1 and the type selection example in Section 6.3) have considerably higher resistance to walker tipover than that predicted by measures proposed in earlier work.

The choice of the appropriate stability measure (Section 6.2) depends on the configuration of the walker and the estimated walker/terrain compliance as described in Section 6.2. Once the appropriate stability measure has been selected, it should be used by the gait planner to plan reliable (i.e., stable) motions (as described in Section 6.3). The predicted stability measure should be compared with the actual stability measure in order to detect potentially anomalous walker–terrain interactions and then activate the appropriate control action (Section 6.3).

We have demonstrated the application of the various stability measures in design, planning, and walking control. Further research in the area of walker stability should focus on implementing these measures in the gait planning and control of a variety of walking machines on a wide variety of terrain types. All four of the stability measures developed here should be monitored and related to walker performance (e.g., tipovers, or near-tipovers that were averted). The results of these experiments should be used to refine the stability measure selection process. The incorporation of the results of the various implementations into the present work will result in a more complete and verified theory that can be used to plan reliable walker motions.

References

Bares, J., Hebert, M., Kanade, T., Krotkov, E., Mitchell, T., Simmons, R., Whittaker, W. L. 1989 (June). AMBLER: An autonomous rover for planetary exploration. *IEEE Computer Magazine*, pp. 18–26.

Hoffman, R. 1991 (December). Autonomous legged robots in agriculture. *Proc. of Automated Agriculture for the 21st Century*. Chicago, Illinois, pp. 218–225.

Hirose, S., Hirose, S., Yaneda, K., Furuya, R., Takagi, T. 1989 (Sept. 4–6). Dynamic and static fusion control of quadruped walking vehicle. *Proc. of IEEE/RSJ Int. Workshop on Intelligent Robots and Systems (IROS '89)*. Tokyo, Japan, pp. 199–203.

Mahalingham, S., and Whittaker, W. L. 1989 (May 7–11). Terrain adaptive gaits for walkers with completely overlapping leg workspaces. *Proc. of Robots 13*. Gaithersburg, MD: Society of Manufacturing Engineers, pp. 6:1–6:14. Reprinted as SME technical paper MS 89-298.

Manko, D. J. 1990. A model of legged locomotion on natural terrain. Ph.D. thesis, Dept. of Civil Engineering, Carnegie Mellon University.

McGhee, R. B., and Frank, A. A. 1968. On the stability properties of quadruped creeping gaits. *Math. Biosci.* 3(3/4):331–351.

Messuri, D. A., and Klein, C. A. 1985. Automatic body regulation for maintaining stability of a legged vehicle during rough terrain locomotion. *IEEE J. Robot. Automation*. RA-1(3):132–141.

Nagy, P. V. 1991. An investigation of walker/terrain interaction. Ph.D. thesis, Dept. of Mechanical Engineering, Carnegie Mellon University.

Nagy, P. V., Desa, S., and Whittaker, W. L. 1992 (Sept. 13–16). Predicting force redistributions on walking robots for reliable locomotion: Modeling and experiments. *Proc. of the 1992 ASME Mechanisms Conference*. Phoenix, AZ: ASME Press, DE-Vol. 45, pp. 573–580.

Nagy, P. V., Whittaker, W. L., and Desa, S. 1992 (May 10–15). A walking prescription for statically stable walkers based on walker/terrain interaction. *Proc. of the 1992 IEEE Robotics and Automation Conference*. Nice, France: IEEE Press, pp. 149–156.

Nagy, P. V., Wu, B. X., and Dowling, K. 1991 (March 19–21). A testbed for attitude control of walking robots. *Proc. of the ISMM Int. Symp. on Computer Applications in Design, Simulation and Analysis*. Las Vegas, NV, pp. 120–123.

Song, S. M., and Waldron, K. J. 1989. *Machines That Walk*. Cambridge, MA: MIT Press.

Zhang, C. D., and Song, S. M. 1989. Gaits and geometry of a walking chair for the disabled. *J. Terramechanics* 26(3/4):211–233.